Journal Article

Characterization of hydrophilic and hydrophobic core-shell microcapsules prepared using a range of antisolvent approaches

Hu, B., Yang, Y., Han, L., Yang, J., Zheng, W., Cao, J.

Food Hydrocolloids 131 (2022) 107750

Contents lists available at ScienceDirect

Food Hydrocolloids

journal homepage: www.elsevier.com/locate/foodhyd

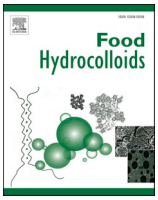

Characterization of hydrophilic and hydrophobic core-shell microcapsules prepared using a range of antisolvent approaches

Bing Hu [a,1], Yisu Yang [b,1], Lingyu Han [a], Jixin Yang [c], Wenjie Zheng [d,**], Jijuan Cao [a,e,*]

[a] Key Laboratory of Biotechnology and Bioresources Utilization of Ministry of Education, School of Life Sciences, Dalian Minzu University, Dalian, 116600, China
[b] Hubei International Scientific and Technological Cooperation Base of Food Hydrocolloids, School of Food and Biological Engineering, Hubei University of Technology, Wuhan, 430068, China
[c] Faculty of Arts, Science and Technology, Wrexham Glyndwr University, Plas Coch, Mold Road, Wrexham, LL11 2AW, United Kingdom
[d] College of Life Science, Tianjin Normal University, Tianjin, 300387, China
[e] Collaborative Innovation Center of Provincial and Ministerial Co-construction for Marine Food Deep Processing, Dalian Polytechnic University, Dalian, 116034, China

ARTICLE INFO

Keywords:
Zein
Core-shell microparticle
Hydrophilic-hydrophobic structure
Restricted antisolvent

ABSTRACT

This study describes three straightforward approaches to leveraging gel network-restricted antisolvent precipitation techniques as a means of preparing hydrophilic hydrophobic core-shell microparticles. Briefly, hydrophilic polysaccharides (sodium alginate (ALG), κ-carrageenan (CAR), and agar (AG)) were utilized to prepare microgel beads that were then immersed in zein solutions (70% ethanol aqueous solution, 70% urea aqueous solution, and zein in 70% acetic acid, respectively), thereby facilitating the controlled, slow antisolvent precipitation of the protein layer on the microbead surfaces and inducing hydrophilic hydrophobic core-shell structure formation. This technique can be readily applied to a range of gelling systems and can be tailored to target particle sizes and shell thicknesses. The resultant core-shell particles offer great promise for controlled delivery of fragrances, drugs, or other bioactive compounds in an application-specific fashion, and can be individually tailored based upon the selected input concentrations and preparation methods. Importantly, this technique is generalizable and can be extended to prepare diverse particles with a range of core-shell structures produced from a wide assortment of hydrophobic materials.

1. Introduction

Composite particles with a core-shell structure are produced using different functionally distinct materials (Wang et al., 2012), and exhibit unique properties attributable to the structural integration of these components (Jaganathan, Madhumitha, & Dhathathreyan, 2013; Yu et al., 2018). The novel physicochemical properties have led to widespread interest in the application of them in materials (Liu, Streufert, et al., 2020), medicine (Martins, Barreiro, Coelho, & Rodrigues, 2014), bioengineering (Kozlowska & Kaczmarkiewicz, 2019), and food industry (He et al., 2018; Hu et al., 2020) contexts. For example, such particles can be utilized to augment the chemical and physical properties of compounds encapsulated therein and regulate the kinetics of their release (Hendrickson, Smith, South, & Lyon, 2010; Kozlovskaya et al., 2014; Liu et al., 2017). Hydrophilic-hydrophobic core-shell microparticles exhibit complementary synergistic functionality as they integrate unique internal and surface materials, offering great promise in a variety of applications (She, Xu, Yin, Tong, & Gao, 2012).

Several approaches to core-shell particle preparation have been reported. For example, Sun, Gao, and Zhong (2018) used a pH-cycle method to generate zein-caseinate core-shell nanoparticles by leveraging the fact that zein and sodium caseinate exhibit differential solubility characteristics. Moreover, using a reverse spherification approach with a reaction-diffusion mechanism, Liu, Liu, Ma, Goff, and Zhong (2020) prepared mechanically-regulated core-shell alginate beads with a spherical structure. An electrospinning strategy has also been adopted by Sun, Guo, Liu, and Yu (2020) to synthesize pullulan-gelatin core-shell nanofibers that exhibited enhanced

* Corresponding author. Key Laboratory of Biotechnology and Bioresources Utilization of Ministry of Education, School of Life Sciences, Dalian Minzu University, Dalian, 116600, China.
** Corresponding author.
E-mail addresses: skyzwj@tjnu.edu.cn (W. Zheng), caojijuan@dlnu.edu.cn (J. Cao).
[1] These authors contributed equally.

https://doi.org/10.1016/j.foodhyd.2022.107750
Received 10 December 2021; Received in revised form 1 March 2022; Accepted 18 April 2022
Available online 2 May 2022
0268-005X/

drug-loading capability while Dai et al. (2018) employed a solvent evaporation technique to generate a zein/propylene glycol alginate core-shell microgel. Additionally, Yang et al. (2014) were able to produce core-shell structures exhibiting dual pH-responsive drug release characteristics by combining microfluidic and electrostatic droplets.

It is worth noting that the above techniques are subject to certain limitations including poor biocompatibility, high costs, and complex preparation protocols. Moreover, they necessitate the use of synthetic materials, thus constraining their applicability in the food, drug, or cosmetic fields. We have previously developed an emulsion templating technique to synthesize hydrophilic-hydrophobic core-shell microcapsules with a controlled size on a microcosmic scale by using core and wall materials consisting of assorted polysaccharides and zein, respectively (Hu et al., 2019). In general, this technique functions due to the solubility of zein in 60–95% (v/v) aqueous solution. However, industrial-scale ethanol utilization entails an inherent fire and explosion risk. Considering the solubility of zein in solutions containing certain acetic acid or urea concentrations, a range of other zein core-shell particle preparation techniques may thus be viable to replace the ethanol-based approaches.

In this work, we aim to develop two new approaches (urea-water antisolvent and acetic acid antisolvent) to hydrophilic-hydrophobic core-shell microcapsule synthesis. These methods can also be generalized to prepare microparticles derived from a diverse array of hydrophilic and hydrophobic materials. To further demonstrate their practical applications, we fabricated edible, biocompatible core-shell microparticles with a hydrophilic core derived from natural food-grade polysaccharides such as alginate (ALG) (Rauner, Meuris, Zoric, & Tiller, 2017), κ-carrageenan (CAR) (Cooke et al., 2018), and agar (AG) (You, Kang, Yin, & Zhang, 2016), together with a hydrophobic shell composed of a prolamin zein (Patel, 2018). These polysaccharides are commonly employed in the biomedical, pharmaceutical, and food industries as gelling, stabilizing, and thickening agents with ideal biodegradability and biocompatibility (Hurtado-López & Murdan, 2005; Pepi & Sudax, 2006). These compounds can undergo sol-gel transitions when exposed to Ca^{2+} ions, K^{+} ions, or upon cooling (Evageliou, Ryan, & Morris, 2019; Lopez-Sanchez, Fredriksson, Larsson, Altskär, & Ström, 2018; Wang et al., 2018). Zein is an FDA-approved, generally recognized as safe (GRAS) corn-derived material (Corradini et al., 2014). It is primarily (>50%) comprised of hydrophobic amino acids (proline, alanine, and leucine) (Patel & Velikov, 2014). Owing to this high content of non-polar amino acids together with the relatively low levels of acidic and basic amino acids, zein is water insoluble but can be solubilized in solutions containing appropriate concentrations of ethanol, urea, or acetic acid (Chen, Ali, et al., 2018). This makes zein ideally suited as a candidate compound for use in the development of colloidal delivery systems to encapsulate drugs (Chen, Han, et al., 2018), nutraceutical compounds (Hu, Wang, Fernandez, & Luo, 2016), pigments (Kasaai, 2018; Patel, Heussen, Dorst, Hazekamp, & Velikov, 2013), and flavoring agents (Chen et al., 2018), or as a tool for altering the visual properties of foods (de Boer, Kok, Imhof, & Velikov, 2018). Herein, we successfully synthesized microcapsules of regulated sizes using hydrogel beads and amphoteric zein, after which a range of microscopic techniques were utilized to assess the microstructural properties of these particles. In addition, the prepared particles were utilized to encapsulate thiamine and ethyl maltol for studies of their *in vitro* digestion and release characteristics.

2. Materials and methods

2.1. Materials

Sodium alginate (G3909401) and κ-carrageenan (Gelcarin GP-911NF) were purchased from FMC BioPolymer (Norway). Agar (1182GR500) was from BioFroxx (Germany). Zein was obtained from Sigma-Aldrich. Acetic acid, urea, ethanol, and calcium carbonate were purchased from Sinopharm Chemical Reagent (Shanghai, China). Mediumchain triglyceride (MCT) was purchased from KLK Oleo (Malaysia). Thiamine and ethyl maltol were purchased from Macklin Reagent (Shanghai, China). Ultrapure water (Milli-Q) water was utilized in all assays.

2.2. Turbidity analyses

Optimal aqueous ethanol, urea, and acetic acid concentrations for use in antisolvent-based microparticle preparation were determined by assessing zein turbidity in solutions containing a range of concentrations of these solvents at 500 nm with a Shimadzu UV-1900 ultraviolet–visible light spectrophotometer (Shimadzu, Japan). Briefly, different amounts of zein were dissolved in a 100% (v/v) ethanol solution, a 19.45 mol/L urea solution, or a 100% (v/v) acetic acid solution for 1 h with constant stirring. Appropriate amounts of deionized water were then added in a dropwise manner with constant stirring (1000 rpm) to yield solutions containing 1% zein and different concentrations of ethanol, urea, or acetic acid. Then a quartz cell with an optical path length of 1 cm was chosen to measure these solutions' turbidities triplicates and reported the average. The turbidity (τ, cm^{-1}) was calculated according to equation (1) (Li, Li, et al., 2012; Li, Fang, et al., 2012):

$$\tau = (1 / L)\ln(I_0 / I_t) \quad (1)$$

where L is the optical path length, I_0 and I_t are the incident and transmitted light intensity, respectively.

2.3. Seeding hydrogel microparticle preparation

Seeding hydrogel microparticles were generated *via* a water-in-oil emulsion template with subsequent internal dispersed phase solidification. Three stock solutions in water were prepared, containing either (1) 3% (w/w) ALG with 50 mM $CaCO_3$, (2) 0.5% (w/w) agar, or (3) 1.5% (w/w) κ-carrageenan. Then 1 part of each stock solution was combined with 4 parts of MCT containing 2% (w/w) L-α-phosphatidylcholine. The mixtures were then emulsified at 200–1000 rpm for 30 min using a low-speed mechanical blender (Eurostar 20 Digital, IKA, Germany) or at 5000–10000 rpm for 3 min with a high-speed homogenizer (T25 digital ULTRA TURRAX®, IKA, Germany) depending on the target particle size. Internal dispersed phase solidification was conducted using different methods. The solidification of ALG seeding microparticles was achieved *via* Ca^{2+} induced gelation. Briefly, one part of MCT containing 3% w/w glacial acetic acid was gradually added to five parts of ALG-in-MCT emulsion, with the acidification-mediated release of calcium ions from $CaCO_3$ triggering ALG gelation. The above experimental steps are carried out at room temperature. Cold-setting was utilized to achieve agar seeding microparticle solidification. Briefly, an agar-in-MCT emulsion was prepared at 95 °C before being rapidly chilled to 4 °C in an ice bath to induce gelation. To solidify κ-carrageenan seeding microparticles, a K^{+}-induced gelation technique was employed. Briefly, one part of MCT was mixed with 2 g of KCl solution (2 M) and then gradually added to five parts of a κ-carrageenan-in-MCT emulsion to drive κ-carrageenan internal phase gelation at room temperature. All solidification was conducted at a constant stirring rate of 50 rpm to ensure that microparticles did not coalesce.

2.4. Hydrophilic-hydrophobic core-shell microparticle fabrication

For ethanol-mediated microparticle fabrication, stock solutions of 0.5%, 1%, 2%, 3%, or 4% (w/v) zein in 70% (v/v) aqueous ethanol were prepared depending on the target shell thickness. The seeding gel microparticle suspensions prepared above were then added to these aqueous zein solutions to induce zein antisolvent precipitation, with the total ethanol concentration being adjusted to 45% (v/v). This antisolvent precipitation process generally proceeded for tens of 30 min

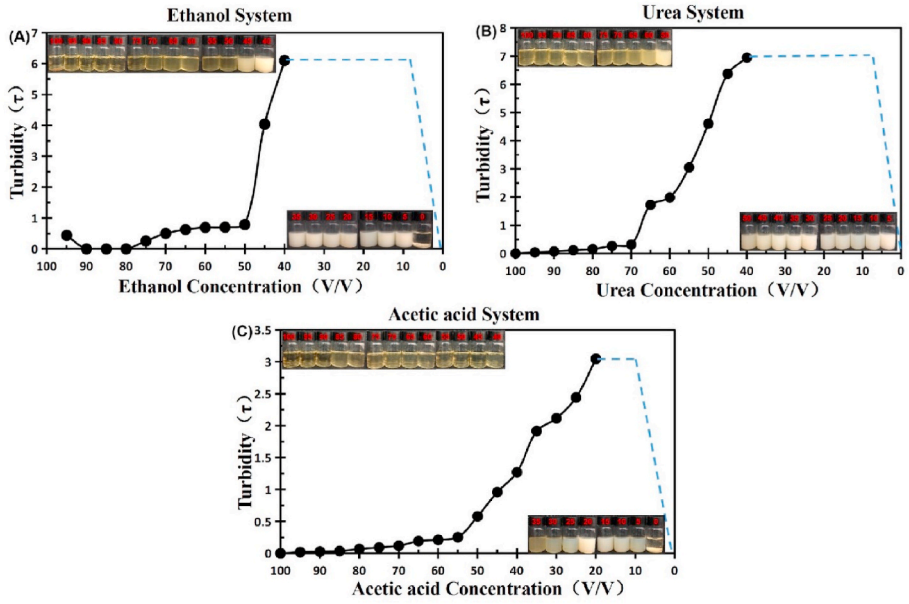

Fig. 1. Zein turbidity changes as a function of antisolvent concentration. (A) The ethanol-water antisolvent system. (B) The urea-water anti-solvent system. (C) The acetic acid-water antisolvent system. Inset: the photographs is macro picture of zein in different concentrations of ethanol urea, acetic acid aqueous solution.

with constant stirring at 50 rpm.

For urea-mediated microparticle fabrication, a 19.45 mol/L urea solution was treated as 100% urea, and a 70% (v/v) aqueous urea stock solution was then used to prepare zein solutions of different concentrations as above. A similar approach to that outlined for the ethanol-based preparation was then taken, with the final urea solution concentration being adjusted to 45% (v/v).

The same approach was also employed using an aqueous acetic acid stock solution (70% v/v), with the final acetic acid content being adjusted to 30% (v/v) after preparation.

2.5. Morphological characterization of core-shell microparticles

2.5.1. Optical microscopy

An Olympus optical microscope (BX50, Olympus, Tokyo, Japan) with a 4 × objective lens was used to image prepared microparticles. Microscopic images were analyzed with the Nano Measurer (v 1.2) software to assess microparticle size distributions, with a minimum of 500 microparticles being randomly selected for each analysis. Data were analyzed with SPSS 23.0 *via* ANOVAs, with $P < 0.05$ as the significance threshold.

2.5.2. Fluorescence microscopy

An IX73 inverted microscope (Olympus, Tokyo, Japan) with a 4 × objective lens was used to image microparticles at an excitation wavelength of 530–550 nm. Rhodamine B (0.1% (v/v)) was used for zein staining.

2.5.3. Confocal laser scanning microscopy (CLSM)

Zein was stained using rhodamine B (0.1% (v/v), after which an inverted laser-scanning confocal microscope (Leica TCS-SP8) with a 10 × objective lens was used to image these particles at an excitation wavelength of 552 nm. Microparticle shell thickness in the resultant images at different locations (>8 per microparticle; >100 total particles) was measured using ImageJ. Data are given as averages with standard deviations, and were analyzed with SPSS 23.0 *via* ANOVAs, with $P < 0.05$ as the significance threshold.

2.5.4. Scanning electron microscopy (SEM)

Microparticle morphology was evaluated *via* field-emission SEM (Helios NanoLab G3, FEI, USA). Briefly, liquid nitrogen was used to freeze microparticles with or without shells, followed by lyophilization. Cross-sectional imaging was conducted by slicing these frozen microparticles with a microtome. Samples were then mounted on a metal stud using double-sided tape, sputter-coated with gold, and imaged at 15 kV in an SEM chamber.

2.6. Thiamine encapsulation and release

Pyridoxine-loaded microparticles were prepared using 3% (w/w) ALG containing 50 mM $CaCO_3$ and 0.1% (w/v) thiamine, according to the method afore-mentioned using a stirring speed of 400 rpm. The microparticles containing thiamine with and without shell were harvested and stored in a concentration of 0.1% (w/v) thiamine to ensure a consistent internal concentration. Thiamine release was measured by mixing 1 g of ALG beads with or without a zein shell in 10 g of water followed by monitoring thiamine absorbance in the aqueous phase at 246 nm at specific time points with a UV–Vis spectrophotometer (TU-1901, Beijing, China) while protected from light. Ultrapure water was used as a control and a standard calibration curve was employed to quantify thiamine release from these particles, which was calculated using Equation (2):

$$\text{Relaease}\ \ (\%) = 100 \times \frac{At}{Ao} \tag{2}$$

where A_t and A_0 respectively correspond to the thiamine concentration released at each time point and the initial concentration of the encapsulated thiamine.

2.7. Ethylmaltol encapsulation and release

An approach similar to that used to prepare thiamine-loaded particles was employed to prepare 0.1% (w/v) ethyl maltol-loaded particles with or without a zein shell using a stirring speed of 400 rpm. Final particles were collected *via* filtration and stored in a 0.1% (w/v) ethyl maltol solution to ensure no loss prior to treatment. A dynamic headspace analysis was utilized to monitor ethyl maltol release. Briefly, 1 g of the prepared ethyl maltol-loaded ALG particles with or without shell was added to an airtight 100 mL bottle at 40 °C, with ethyl maltol release amounts and release rates being assessed by collecting a gas sample (1

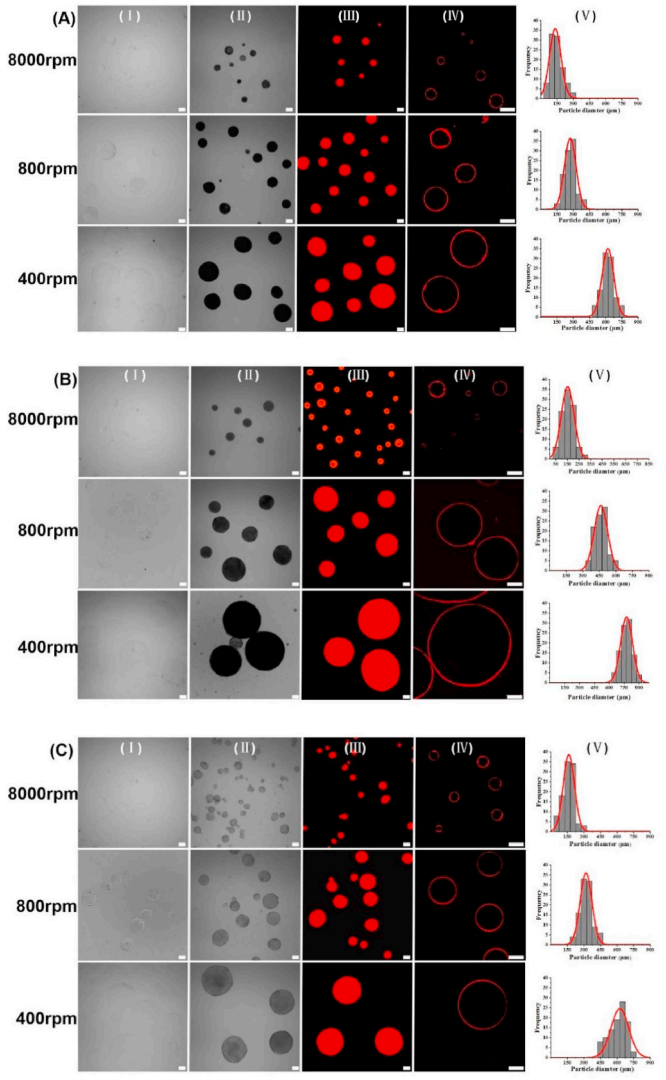

Fig. 2. ALG-Zein core-shell particle morphological profiles for particles prepared using the (A) ethanol-water, (B) urea-water, and (C) acetic acid-water antisolvent systems. Colloid particles without zein are shown in Column I, while Column II shows microscopic images of core-shell structured particles, Column III shows fluorescence images of core-shell structured particles, Column IV shows CLSM images of these particles, and Column V shows particle size maps for the prepared particles. Scale bars: 200 μm. Images in separate columns were not taken from the same microparticle samples.

mL) from the headspace every 90 s and injecting it into a gas chromatography (GC) system (Agilent 7890B).

3. Results and discussion

3.1. Zein solubility characterization

Zein can readily be dissolved in a variety of organic solvents such as aqueous ethanol, thermal glycerol, propylene glycol, and dimethylformamide, in addition to being soluble in specific urea and acetic acid concentrations (Li, Li, et al., 2012; Li, Xia, Shi, & Huang, 2011). Zein solubility changes with variations in ethanol, acetic acid, and urea concentrations. Consistently, we found that zein suspension turbidity rose with decreasing ethanol concentrations in an aqueous solution from 75% (Fig. 1A), while in a urea-water solution zein turbidity rose as the urea concentration decreased from 80% (Fig. 1B), and zein turbidity increased in an acetic acid-water solution as the acetic acid concentration fell from 80 to 20% (Fig. 1C). At ethanol, urea, and acetic acid concentrations below these respective lower limits, substantial agglomeration and precipitation were observed. Such aggregation and unregulated assembly are not desirable. On the other hand, at ethanol, urea, and acetic acid concentrations above these respective lower limits, it was observed that a large amount of protein was still in solution and the antisolvent approach was incapable to form a complete protein shell layer. Therefore, these experiments revealed that 45% ethanol-water, 45% urea-water, and 30% acetic acid-water solutions were suitable for use in the context of antisolvent-based microparticle assembly.

3.2. Core-shell particle morphological characterization

3.2.1. Regulation of microparticle size and shell thickness

Next, ALG-zein hydrophilic-hydrophobic core-shell particles were prepared using these three different antisolvent techniques, with images of the resultant particles being shown in Fig. 2(A)–(C). Prepared ALG particles were initially transparent when visualized (Fig. 2I), but became opaque following core-shell structure formation (Figure.2II). This result was attributable to the formation of a precipitated dense zein shell on ALG particle surfaces. Fluorescent and CLSM imaging reveals the zein protein shells of these particles to be well-defined and uniform (Fig.2III and IV). Shell layers were successfully established on ALG particle surfaces using all three antisolvent precipitation strategies, yielding the desired core-shell structure particles (see Fig. 3).

In addition, we assessed our ability to finely control the size of the prepared hydrophilic hydrophobic core-shell microparticles by measuring the particle size distributions for >100 particles per sample with the Nano Measurer (v1.2). As shown in Fig. 2V, particle size was readily adjustable from tens to hundreds of microns in diameter by modulating the stirring/homogenization speed. Irrespective of microparticle size, a well-defined zein protein shell remained evident on the prepared particles. All three antisolvent techniques were sufficient to adjust zein shell thickness by altering zein initial concentrations, with a uniform shell layer being formed at a 2% (w/v) zein concentration. Stirring/homogenization speed significantly impacted the mean size of the prepared core-shell particles (Table 1), while zein concentration significantly affected shell thickness. Owing to the limited scalability of emulsification-based particle preparation, only micron-scale core-shell particles were generated in the present study. However, further research using smaller seed hydrogel particles and inverse solvent precipitation methods that take gel network limitations into account is also warranted as these strategies should be well-suited to core-shell microparticle preparation.

Meanwhile, shell thickness of particles prepared using each of the three antisolvent systems at different zein concentrations was measured by analyzing CLSM images using Image J software. The shell thickness was determined at different locations of the shell profile (>8 for a single microparticle) and over a sufficient number of microparticles (>100). Average values with standard deviation were reported. The analysis showed that uniform and complete protein shell layers were obtained at 2% concentration of zein in all three systems, where the thickness of the particle shell prepared in the ethanol system was greater than that of the particles prepared in the urea system and the thickness of the particle shell prepared in the acetic acid system was the thinnest for the same protein concentration. At zein concentrations from 1% to 4%, the shell thickness of the prepared particles increased accordingly.

3.2.2. Microparticle morphological analyses

Hydrophilic-hydrophobic core-shell structured ALG particle morphology following antisolvent precipitation using the three methods outlined above was assessed *via* field-emission SEM (Fig. 4). Particles both with (Fig. 4II) and without a shell (Fig. 4I) were spherical, and the zein-coated ALG particles exhibited a rougher surface (Fig. 4II) than that of ALG hydrophilic nucleosomes (Fig. 4I). This suggests that individual zein clusters underwent nucleation and swelling on seed hydrogel

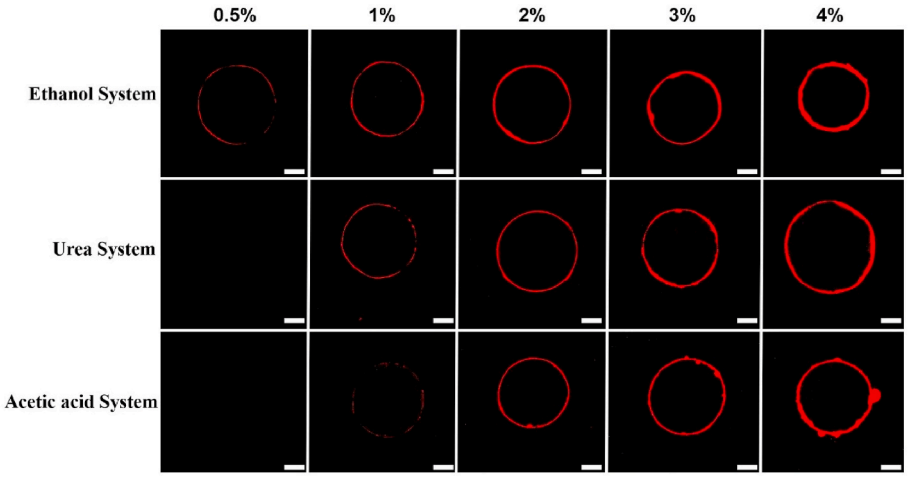

Fig. 3. CLSM images of ALG-Zein core-shell particles generated using the three indicated antisolvent systems with a range of zein concentrations. Scale bars: 200 μm.

Table 1
Control of ALG-Zein core-shell microparticle size and shell thickness by regulating zein concentrations and stirring/homogenization speed during emulsification.

Anti-solvent System	Zein (% w/v)	Stirring speed (rpm)	Average particle size (μm)	Average shell thickness (μm)
Ethanol System	1.0	$400^{I)}$	539.9 ± 14.2^{a}	11.5 ± 0.2^{A}
	2.0	$400^{I)}$	545.5 ± 18.8^{a}	23.6 ± 0.7^{B}
	3.0	$400^{I)}$	549.3 ± 16.3^{a}	28.0 ± 0.9^{C}
	4.0	$400^{I)}$	553.3 ± 14.6^{a}	33.6 ± 0.9^{D}
	2.0	$800^{I)}$	322.5 ± 13.5^{b}	14.6 ± 0.4^{B}
	2.0	$8000^{II)}$	164.3 ± 16.8^{c}	9.8 ± 0.2^{B}
Urea System	1.0	$400^{I)}$	765.9 ± 12.7^{a}	9.5 ± 0.3^{A}
	2.0	$400^{I)}$	779.5 ± 13.4^{a}	17.4 ± 0.7^{B}
	3.0	$400^{I)}$	784.5 ± 16.7^{a}	23.3 ± 1.2^{C}
	4.0	$400^{I)}$	788.5 ± 17.4^{a}	30.4 ± 0.7^{D}
	2.0	$800^{I)}$	425.5 ± 17.5^{b}	11.6 ± 0.4^{B}
	2.0	$8000^{II)}$	154.5 ± 19.8^{c}	8.8 ± 0.4^{B}
Acetic acid System	1.0	$400^{I)}$	603.9 ± 13.7^{a}	7.5 ± 0.4^{A}
	2.0	$400^{I)}$	621.7 ± 14.5^{a}	14.7 ± 0.9^{B}
	3.0	$400^{I)}$	631.7 ± 13.2^{a}	21.6 ± 0.6^{C}
	4.0	$400^{I)}$	637.7 ± 12.3^{a}	29.4 ± 0.5^{D}
	2.0	$800^{I)}$	271.5 ± 14.5^{b}	8.6 ± 0.8^{B}
	2.0	$8000^{II)}$	146.3 ± 12.8^{c}	6.9 ± 0.6^{B}

I) achieved with a low-speed mechanical blender; II) achieved with a high-speed homogenizer. Through significant analysis , A,B,C,D indicate that zein concentrations significantly affected average shell thickness. a,b,c,d indicate that stirring speed significantly affected the average particle size.

particle surfaces, ultimately aggregating into a structurally continuous shell layer. All three antisolvent systems yielded distinct nucleation-shell structured particles.

SEM images of particle cross-sections confirmed the presence of the expected core-shell structures (Fig. 4III and 4IV). Hydrophilic nucleosomes exhibit a hollow, spongy structure, whereas protein shells exhibit a more compact and solid appearance. The spongy structures were attributed to the characteristics of the hydrogel network following freeze-drying and dehydration. The dense shell structure is distinct from the porous structure associated with conventional antisolvent precipitations, suggesting that slower adsorption kinetics may result in more compact protein deposition. The shell layer of particles prepared *via* an ethanol antisolvent method was substantially coarser than those of particles prepared *via* the urea and acetic acid antisolvent methods.

3.3. Generalizability of antisolvent preparation techniques

Using ALG as a hydrophilic core, we successfully prepared core-shell microparticles with controllable size and shell thickness. To confirm the generalizability of these methods and associated findings, we next utilized hydrophilic cores composed of agar and κ-carrageenan that were respectively treated to form gels *via* cooling and K^{+} ion exposure to prepare core-shell microparticles using the same antisolvent methods. Images of particles prepared using an agar-based hydrophilic core are shown in Fig. 5A. While the uncoated agar particles were transparent under light microscopy (Fig. 5A–I), they grew opaque following core-shell structure formation due to the dense zein coating (Fig. 5A–II). The resultant protein shell layer appeared relatively uniform and well-defined upon fluorescence and laser confocal microscopy imaging (Fig. 5A–III and 5-IV), and all three antisolvent techniques yielded similar agar-zein core-shell structured particles. Similarly, κ-carrageenan gel particles were initially transparent (Fig. 5B–I), then opaque following core-shell formation (Fig. 5B–II). The observed trends in shell thickness were similar to those observed for ALG-zein and AG-zein core-shell particles under these three antisolvent systems, with well-defined, uniform protein shells being evident upon fluorescence microscopy and laser confocal microscopy imaging (Fig. 5B–III and 5B-IV). As shells were successfully established on the surfaces of all three hydrogels when using three different gelation techniques, these methods can be universally applied to generate hydrogels from a range of materials.

3.4. Release of encapsulated thiamine from core-shell particles

Next, we explored the dynamics of controlled thiamine release when using core-shell particles with different thicknesses prepared *via* the different antisolvent methods discussed above (Fig. 6). For ALG microcapsules containing thiamine prepared using the ethanol system, thiamine release rates reached 80% within 60 min in the absence of a zein shell, whereas these rates fell to <50% and <25%, respectively, when a zein shell was added to these particles using a 1% or 2% zein concentration. Similar results were also obtained for thiamine-containing ALG microcapsules prepared using the urea- and acetic acid-based systems (Table 2) (see Fig. 7).

These results indicate that the core-shell microcapsules synthesized using these three antisolvent precipitation techniques can be effectively leveraged to facilitate the controlled, gradual release of functional materials, with the modulation of zein concentrations having the potential to alter shell thickness and consequent thiamine release rates. In addition, application-specific antisolvent strategies can be used to prepare appropriate core-shell microcapsules, making this technique of clear value in the sustained release of food or drug compounds.

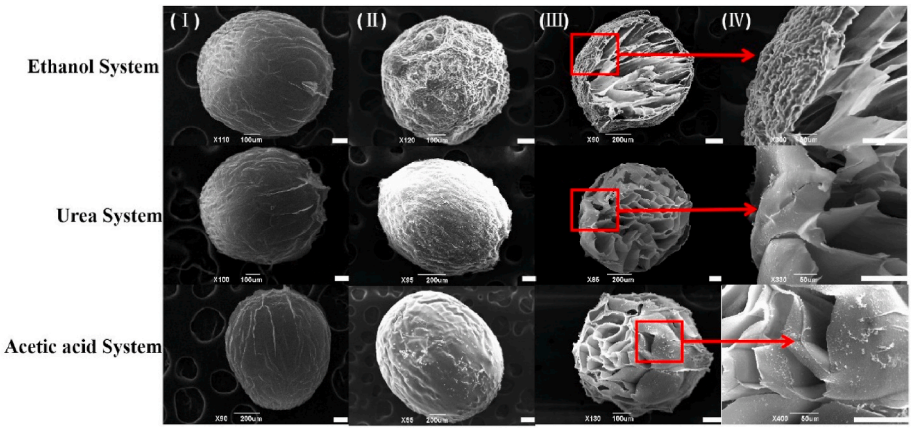

Fig. 4. Representative SEM images of freeze-dried alginate hydrogel microparticles without (I) and with (II) zein shells. Cross-sectional SEM images of these particles are shown in (III), with indicated areas being enlarged in (IV). Scale bars: 100 μm.

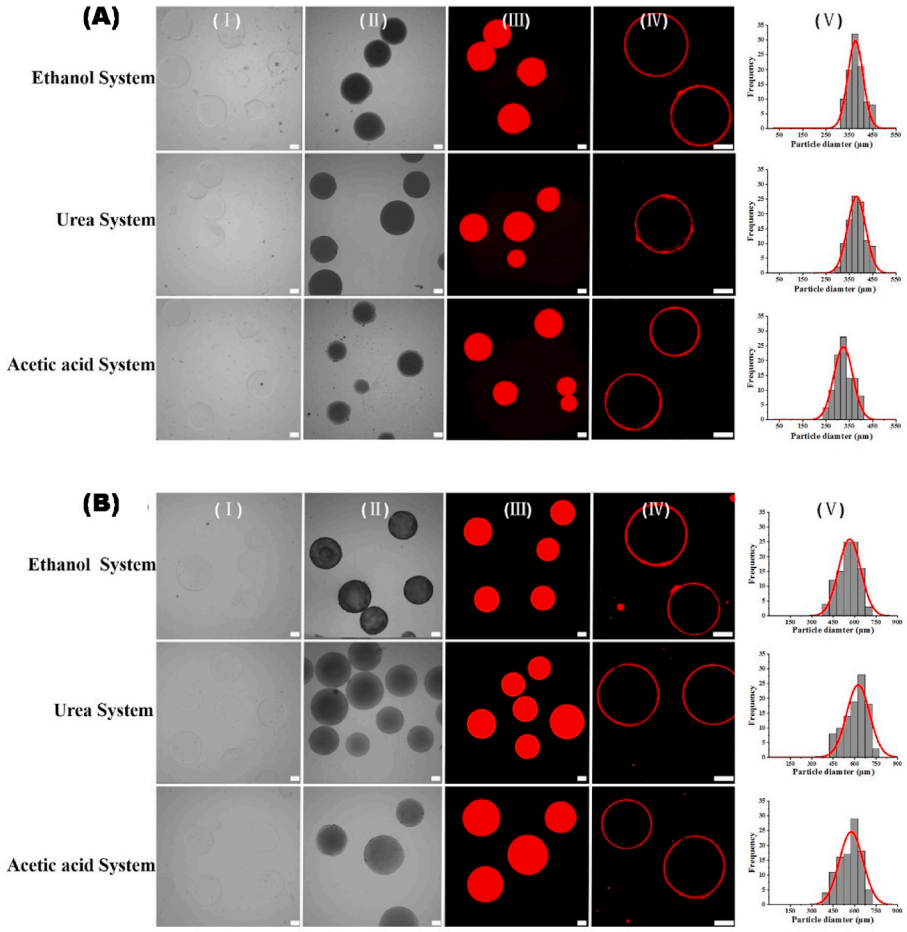

Fig. 5. Morphological characterization of the core-shell particles using agar (A) and κ-carrageenan (B) prepared *via* the three different antisolvent methods. Pure colloidal particles are shown in Column I, while Column II shows microscopic images of core-shell particles, Column III shows fluorescence images of core-shell particles, Column IV shows CLSM images of core-shell particles, and Column V shows the size distributions of these core-shell particles. Images in separate columns were not taken from the same microparticle samples. Scale bars: 200 μm.

3.5. Release of encapsulated ethyl maltol from core-shell particles

Next, ALG-zein core-shell particles encapsulating 0.1% w/v ethyl maltol were prepared using these three different antisolvent precipitation strategies, with release rates being normalized to an equilibrium headspace concentration of 0.1% w/v ethyl maltol in aqueous solutions. Average shell thickness values for core-shell microparticles prepared with 2.0% (w/v) zein using the ethanol, urea, and acetic acid antisolvent precipitation methods were 23.6, 17.4, and 14.7 μm, respectively (Table 1). Ethyl maltol release was dependent upon shell thickness, and was relatively rapid during the initial stage before reaching pseudo-equilibrium after about 10 min. As shell thickness rose from 0 (ALG only), to 14.7 μm (acetic acid), 17.4 μm (urea), and 23.6 μm (ethanol), the equilibrium release rates decreased from 80% to 50%, 38% and 34%. Slight decreases in release rates at later time points may be a consequence of the persistent headspace GC sampling, reducing equilibrium concentrations in this assay system, as observed previously by Chen et al. (Chen, Guo, Wang, Yin, & Yang, 2016).

Overall, the results of this study clearly demonstrate that all three antisolvent precipitation approaches can be utilized to prepare

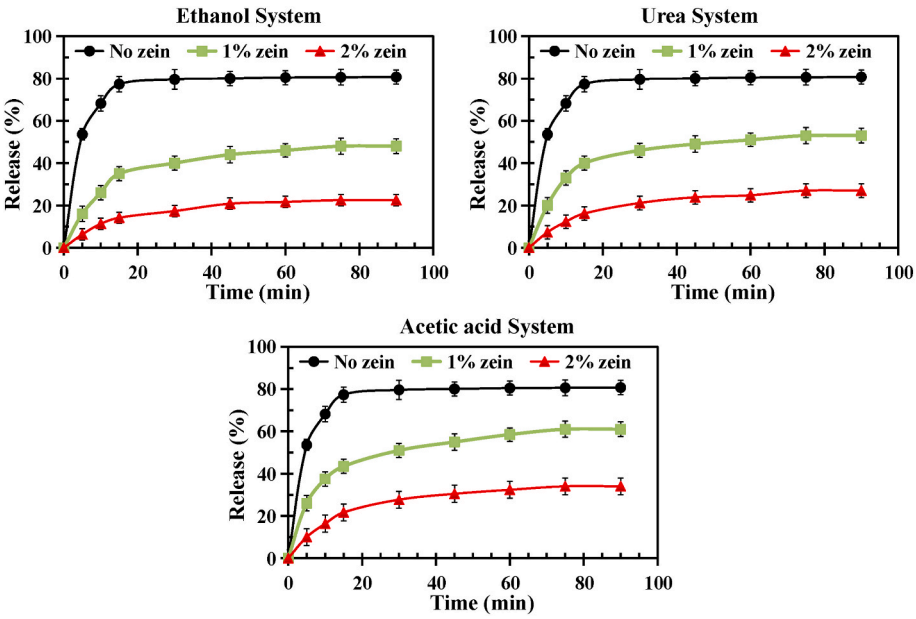

Fig. 6. Thiamine release curves for ALG microcapsules and core-shell microcapsules.

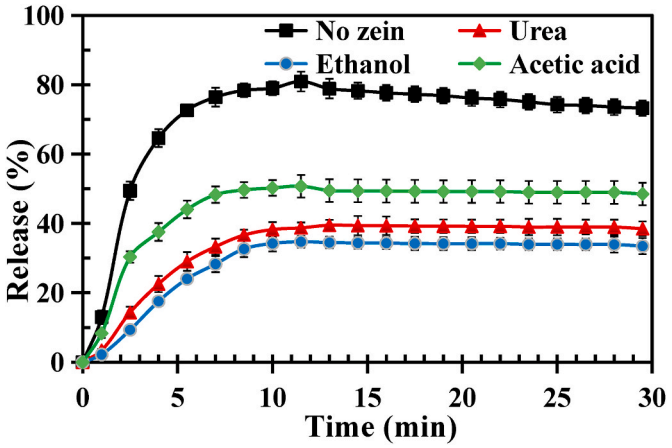

Fig. 7. Release profiles for ethyl maltol-containing ALG microcapsules and core-shell microcapsules.

Table 2
Thiamine release rates for ALG microcapsules and core-shell microcapsules.

Anti-solvent System	Zein (% w/v)	Average shell thickness (μm)	Release time (min)	Release rate (%)
Ethanol System	0	0	60	80 ± 3.3
	1.0	23.6 ± 0.7	60	50 ± 3.1
	2.0	28.0 ± 0.9	60	23 ± 2.8
Urea System	0	0	60	80 ± 3.3
	1.0	17.4 ± 0.7	60	53 ± 3.2
	2.0	23.3 ± 1.2	60	27 ± 3.4
Acetic acid System	0	0	60	80 ± 3.9
	1.0	14.7 ± 0.9	60	60 ± 4.2
	2.0	21.6 ± 0.6	60	34 ± 5.2

hydrophilic-hydrophobic core-shell microparticles encapsulating volatile substances to protect them and ensure their controlled release.

4. Conclusions

In summary, in the present study, hydrophilic-hydrophobic core-shell particles were successfully synthesized using a combination of hydrophilic polysaccharides and hydrophobic zein *via* emulsion templating with three different antisolvent precipitation techniques. Core-shell particles of varying diameter and thickness were prepared by modulating stirring rates and zein concentrations. Prepared core particles were coated with a dense, uniform zein layer that was integral to the controlled release of thiamine and ethyl maltol from these particles. Moreover, these techniques are highly adaptable and can be employed in a range of applications. Owing to the simplicity of this formulation strategy and the unique structural characteristics of the resultant particles, this approach offers great promise for use in biomedical, cosmetic, and culinary contexts.

Author statement

Bing Hu: Conceptualization, Methodology, Investigation, Formal Analysis, Writing - Original Draft;
Yisu Yang: Data Curation, Software, Writing - Original Draft;
Lingyu Han: Visualization, Investigation;
Jixin Yang: Resources, Supervision, Software, Validation;
Wenjie Zheng: Visualization, Writing - Review & Editing.
Jijuan Cao (Corresponding Author): Conceptualization, Funding Acquisition, Resources, Supervision, Writing - Review & Editing.

Declaration of competing interest

The authors declare that they have no known competing financial interests or personal relationships that could have appeared to influence the work reported in this paper.

Acknowledgements

This article was funded by the National Key Research and Development Project (2021YFF0601900), Liaoning Provincial Science and Technology Innovation Leading Talents Project (XLYC2002106),

Natural Science Foundation of Liaoning Province (2021-MS-147), Dalian High-Level Talent Innovation, Scientific and Technological Talent Entrepreneurship and Innovation Team Support Projects in Key Fields (2020RQ122), Liaoning Province Livelihood Science and Technology Project (2021JH2/10200019), Department of Education of Liaoning Province (LJKZ0037), Dalian Key Science And Technology Project (2021JB12SN038).

Abbreviations

ALG	Sodium alginate
CAR	κ-carrageenan
MCT	Medium-chain triglyceride
CLSM	Confocal scanning laser microscope
SEM	Scanning electron microscopy
GC	Gas chromatograph

References

de Boer, F. Y., Kok, R. N. U., Imhof, A., & Velikov, K. P. (2018). White zein colloidal particles: Synthesis and characterization of their optical properties on the single particle level and in concentrated suspensions. *Soft Matter, 14*(15), 2870–2878.

Chen, G., Ali, F., Dong, S., Yin, Z., Li, S., & Chen, Y. (2018). Preparation, characterization and functional evaluation of chitosan-based films with zein coatings produced by cold plasma. *Carbohydrate Polymers, 202*, 39–46.

Chen, X.-W., Guo, J., Wang, J.-M., Yin, S.-W., & Yang, X.-Q. (2016). Controlled volatile release of structured emulsions based on phytosterols crystallization. *Food Hydrocolloids, 56*, 170–179.

Chen, S., Han, Y., Sun, C., Dai, L., Yang, S., Wei, Y., et al. (2018). Effect of molecular weight of hyaluronan on zein-based nanoparticles: Fabrication, structural characterization and delivery of curcumin. *Carbohydrate Polymers, 201*, 599–607.

Chen, Y., Shu, M., Yao, X., Wu, K., Zhang, K., He, Y., et al. (2018). Effect of zein-based microencapsules on the release and oxidation of loaded limonene. *Food Hydrocolloids, 84*, 330–336.

Cooke, M. E., Jones, S. W., Ter Horst, B., Moiemen, N., Snow, M., Chouhan, G., et al. (2018). Structuring of hydrogels across multiple length scales for biomedical applications. *Advanced Materials, 30*(14), Article e1705013.

Corradini, E., Curti, P. S., Meniqueti, A. B., Martins, A. F., Rubira, A. F., & Muniz, E. C. (2014). Recent advances in food-packing, pharmaceutical and biomedical applications of zein and zein-based materials. *International Journal of Molecular Sciences, 15*(12), 22438–22470.

Dai, L., Zhan, X., Wei, Y., Sun, C., Mao, L., McClements, D. J., et al. (2018). Composite zein - propylene glycol alginate particles prepared using solvent evaporation: Characterization and application as Pickering emulsion stabilizers. *Food Hydrocolloids, 85*, 281–290.

Evageliou, V. I., Ryan, P. M., & Morris, E. R. (2019). Effect of monovalent cations on calcium-induced assemblies of kappa carrageenan. *Food Hydrocolloids, 86*, 141–145.

Hendrickson, G., Smith, M., South, A., & Lyon, L. (2010). Design of multiresponsive hydrogel particles and assemblies. *Advanced Functional Materials, 20*, 1697–1712.

He, T., Xu, X., Ni, B., Lin, H., Li, C., Hu, W., et al. (2018). Metal-organic framework based microcapsules. *Angewandte Chemie International Edition, 57*, 10148–10152.

Hu, B., Han, L., Ma, R., Phillips, G. O., Nishinari, K., & Fang, Y. (2019). All-natural food-grade hydrophilic-hydrophobic core-shell microparticles: Facile fabrication based on gel-network-restricted antisolvent method. *ACS Applied Materials & Interfaces, 11*(12), 11936–11946.

Hu, Y., Li, C., Wang, J., Jia, X., Zhu, J., Wang, Q., et al. (2020). Osmosis manipulable morphology and photonic property of microcapsules with colloidal nano-in-micro structure. *Journal of Colloid and Interface Science, 574*, 337–346.

Hurtado-López, P., & Murdan, S. (2005). Formulation and characterisation of zein microspheres as delivery vehicles. *Journal of Drug Delivery Science and Technology, 15*(4), 267–272.

Hu, S., Wang, T., Fernandez, M. L., & Luo, Y. (2016). Development of tannic acid cross-linked hollow zein nanoparticles as potential oral delivery vehicles for curcumin. *Food Hydrocolloids, 61*, 821–831.

Jaganathan, M., Dhanasekaran, M., & Dhathathreyan, A. (2013). Protein microcapsules: Preparation and applications. *Advances in Colloid and Interface Science, 209*.

Kasaai, M. R. (2018). Zein and zein -based nano-materials for food and nutrition applications: A review. *Trends in Food Science & Technology, 79*, 184–197.

Kozlovskaya, V., Alexander, J. F., Wang, Y., Kuncewicz, T., Liu, X., Godin, B., et al. (2014). Internalization of red blood cell-mimicking hydrogel capsules with pH-triggered shape responses. *ACS Nano, 8*(6), 5725–5737.

Kozlowska, J., & Kaczmarkiewicz, A. (2019). Collagen matrices containing poly(vinyl alcohol) microcapsules with retinyl palmitate – structure, stability, mechanical and swelling properties. *Polymer Degradation and Stability, 161*, 108–113.

Li, X., Fang, Y., Al-Assafs, et al. (2012). Complexation of bovine serum albumin and sugar beet pectin: Structural transitions and phase diagram. *Langmuir, 28*(27), 10164–10176, 2012.

Li, Y., Li, J., Xia, Q., Zhang, B., Wang, Q., & Huang, Q. (2012). Understanding the dissolution of α-zein in aqueous ethanol and acetic acid solutions. *Journal of Physical Chemistry B, 116*(39), 12057–12064.

Liu, H., Liu, F., Ma, Y., Goff, H. D., & Zhong, F. (2020). Versatile preparation of spherically and mechanically controllable liquid-core-shell alginate-based bead through interfacial gelation. *Carbohydrate Polymers, 236*, Article 115980.

Liu, J., Streufert, J., Mu, K., Si, T., Han, T., Han, Y., et al. (2020). Polymer composites containing phase-change microcapsules displaying deep undercooling exhibit thermal history-dependent mechanical properties. *Advanced Materials Technologies, 5*, Article 2000286.

Liu, X., Zheng, H., Li, G., Li, H., Zhang, P., Tong, W., et al. (2017). Fabrication of polyurethane microcapsules with different shapes and their influence on cellular internalization. *Colloids and Surfaces B: Biointerfaces, 158*, 675–681.

Li, Y., Xia, Q., Shi, K., & Huang, Q. (2011). Scaling behaviors of α-zein in acetic acid solutions. *Journal of Physical Chemistry B, 115*(32), 9695–9702.

Lopez-Sanchez, P., Fredriksson, N., Larsson, A., Altskär, A., & Ström, A. (2018). High sugar content impacts microstructure, mechanics and release of calcium-alginate gels. *Food Hydrocolloids, 84*, 26–33.

Martins, I. M., Barreiro, M. F., Coelho, M., & Rodrigues, A. E. (2014). Microencapsulation of essential oils with biodegradable polymeric carriers for cosmetic applications. *Chemical Engineering Journal, 245*, 191–200.

Patel, A. (2018). Functional and engineered colloids from edible materials for emerging applications in designing the food of the future. *Advanced Functional Materials, 30*.

Patel, A. R., Heussen, P. C. M., Dorst, E., Hazekamp, J., & Velikov, K. P. (2013). Colloidal approach to prepare colour blends from colourants with different solubility profiles. *Food Chemistry, 141*(2), 1466–1471.

Patel, A. R., & Velikov, K. P. (2014). Zein as a source of functional colloidal nano- and microstructures. *Current Opinion in Colloid & Interface Science, 19*(5), 450–458.

Pepi, H. L., & Sudax, M. (2006). Zein microspheres as drug/antigen carriers: A study of their degradation and erosion, in the presence and absence of enzymes. *Journal of Microencapsulation, 23*(3), 303–314.

Rauner, N., Meuris, M., Zoric, M., & Tiller, J. C. (2017). Enzymatic mineralization generates ultrastiff and tough hydrogels with tunable mechanics. *Nature, 543*(7645), 407–410.

She, S., Xu, C., Yin, X., Tong, W., & Gao, C. (2012). Shape deformation and recovery of multilayer microcapsules after being squeezed through a microchannel. *Langmuir, 28*(11), 5010–5016.

Sun, C., Gao, Y., & Zhong, Q. (2018). Effects of acidification by glucono-delta-lactone or hydrochloric acid on structures of zein-caseinate nanocomplexes self-assembled during a pH cycle. *Food Hydrocolloids, 82*, 173–185.

Sun, F., Guo, J., Liu, Y., & Yu, Y. (2020). Preparation and characterization of poly(3-hydroxybutyrate-co-4-hydroxybutyrate)/pullulan-gelatin electrospun nanofibers with shell-core structure. *Biomedical Materials, 15*, Article 045023.

Wang, Y.-F., Shao, J.-J., Zhou, C.-H., Zhang, D.-L., Bie, X.-M., Lv, F.-X., et al. (2012). Food preservation effects of curcumin microcapsules. *Food Control, 27*(1), 113–117.

Wang, Z., Yang, K., Li, H., Yuan, C., Zhu, X., Huang, H., et al. (2018). In situ observation of sol-gel transition of agarose aqueous solution by fluorescence measurement. *International Journal of Biological Macromolecules, 112*, 803–808.

Yang, C. H., Wang, C. Y., Grumezescu, A. M., Wang, A. H., Hsiao, C. J., Chen, Z. Y., et al. (2014). Core-shell structure microcapsules with dual pH-responsive drug release function. *Electrophoresis, 35*(18), 2673–2680.

You, B., Kang, F., Yin, P., & Zhang, Q. (2016). Hydrogel-derived heteroatom-doped porous carbon networks for supercapacitor and electrocatalytic oxygen reduction. *Carbon, 103*, 9–15.

Yu, M., Xu, L., Tian, F., Su, Q., Zheng, N., Yang, Y., et al. (2018). Rapid transport of deformation-tuned nanoparticles across biological hydrogels and cellular barriers. *Nature Communications, 9*.